Int. J. Heat Mass Transfer. Vol. 18, pp. 917–926. Pergamon Press 1975. Printed in Great Britain

HEAT-TRANSFER CHARACTERISTICS OF A BUBBLE-INDUCED WATER JET IMPINGING ON AN ICE SURFACE

YIN-CHAO YEN*
U.S. Army Cold Regions Research and Engineering Laboratory, Hanover, New Hampshire 03755, U.S.A.

(*Received* 16 *July* 1974)

Abstract—An experimental study on the heat-transfer characteristics of a bubble-driven water jet impinging on an ice surface was conducted. Two Lucite columns, one 1·829 m high and 0·286 m in diameter, and the other 1·219 m high and 0·140 m in diameter were used. Water levels were maintained at 0·762 and 1·524 m in the large column and 0·840 m in the small column. Hypodermic needles with openings 0·152, 0·406 and 0·838 mm were used in bubble formation covering a volumetric air flow rate from $7{\cdot}39 \times 10^{-8}$ to $9{\cdot}91 \times 10^{-7}$ m^3/s. To simulate winter environmental conditions in Northern America, the water temperature at the column bottom was thermostatically maintained at its temperature of maximum density, i.e. about 4°C. Cylindrical blocks of ice having diameters slightly less than those of the columns were supported at the column top while maintaining a proper immersion of the melting surface in the water level. The experimental results can be well represented by

$$Nu = 630(d_n)^{0.4}(Re_n)^{0.391} \quad (1)$$

for $8 < Re_n < 10^3$. The Nu is defined in terms of heat-transfer coefficient over the sample cross sectional area, the sample diameter, and thermal conductivity of water, and Re_n is defined in terms of the air flow characteristics at the nozzle exit. The effect of both water levels and column diameter were found to be absent in the correlation.

Using a Reynolds number based on the bubble-induced water jet flow characteristics, the experimental results were compared with the limited results reported on heat transfer between a round air jet and a plane surface held normal to the jet flow (modified to apply to water flow). The least-square analysis expression,

$$Nu = 0{\cdot}00010(D_s)^{-1{\cdot}2}(Re_a)^{1{\cdot}311} \quad (2)$$

indicating the absences of both nozzle diameter and height of water level, was found to represent the data extremely well. The above expression under- and overestimates Nu for lower and higher Re_a values than those predicted from the expression representing pure water jet $Nu = 1{\cdot}94(Re_a)^{0.55}$. However, in view of the numerous assumptions and wide differences in experimental parameters, the agreement is still considered to be remarkably good.

NOMENCLATURE

A, sample cross-sectional area;
C, rate of spread of velocity profile;
c, heat capacity;
D, column diameter;
D_i, diameter of area of impingement;
D_s, sample diameter or diameter of heat-transfer area;
d_b, equivalent bubble diameter;
d_n, nozzle diameter;
f_b, bubble frequency;
G, force per unit height imposed in the liquid;
h, average heat-transfer coefficient over the heat-transfer surface;
h_i, average heat-transfer coefficient based on the area corresponding to the area of impingement;
k, thermal conductivity;
L, water depth, axial distance from nozzle tip to sample surface;
L_i, latent heat of fusion;
L^*, defined as $L + P_{atm}/\gamma_w$;
M_s, sample weight at the completion of experiment;
Nu, Nusselt number defined as hD_s/k_w;
Nu_i, Nusselt number defined as h_iD_i/k_w;
Nu_n, Nusselt number defined as hd_n/k_w;
P_{atm}, atmospheric pressure;
Q_m, heat exchange associated with melting;
Q_s, sensible heat change of the remaining sample;
$q(\theta)$, heat flux;
R, column radius, Rotameter setting;
r, coordinate in radial direction;
Re_a, Reynolds number defined as D_sv_c/v_w;
Re_i, Reynolds number defined as D_iv_c/v_w;
Re_n, Reynolds number defined as d_nv_a/v_a;
T_b, bulk water temperature;
T_f, freezing temperature;
T_i, initial ice temperature;
ΔT, defined as $T_b - T_f$;
ΔT_b, temperature differences near the melting surface at the start and completion of the experiment;
V_a, volumetric flow rate;
v_a, air velocity at nozzle exit;
v_b, mean bubble stream velocity;
v_c, vertical centerline water velocity;

* Also Visiting Professor of Chemical Engineering, University of New Hampshire, Durham, NH, U.S.A.

v_w, vertical water velocity;
W_i, weight of ice melted;
y, coordinate in vertical direction.

Greek symbols

γ_w, specific weight;
μ, viscosity;
ν, kinematic viscosity;
π, constant;
ρ, density;
θ, time;
θ_p, freezing period.

Subscripts

a, air;
b, bubble, bottom;
c, center;
f, freezing;
i, ice, impingement;
n, nozzle;
o, origin;
s, sensible;
t, top;
w, water.

INTRODUCTION

WINTER, with its freezing temperatures, has posed many problems in cold regions for navigation, and maintenance of structures located in water. During long, cold winters many lakes, harbors, ports, and rivers become covered with ice which greatly shortens the navigation period and thus affects the economic situation in these areas. In attempting to solve this problem, air-bubbler devices have been developed which operate on the principle that subsurface warm water can be brought to the surface by a stream of air bubbles rising through the otherwise quiescent bodies of water. The first air bubbler system was installed in 1917 at the Keokuk Dam [1], and since that time a number of similar usages have been reported [2], and a general discussion on the use of air bubblers as ice control devices can be found in a monograph by Michel [3].

In the natural environment, the necessary condition for a successful operation of an air-bubbler system is the presence of the heat reservoir of the water body itself, which must be at least equal to or greater than the net heat loss at the water surface resulting from a combination of exchange processes, i.e. evaporation, condensation, net short and long wave radiative, and convective heat transfer. This condition for the entire freezing period can be expressed as

$$\int_0^L c_w \rho_w (T - T_f) \mathrm{d}y = \int_0^{\theta_p} q(\theta)\, \mathrm{d}\theta \qquad (3)$$

in which L is water depth above the air source in the y-direction, c_w, ρ_w and T are the heat capacity, density and temperature of water, T_f is the freezing temperature of water which is usually at 0°C, $q(\theta)$ is the surface heat flux as a function of time θ, and θ_p is the freezing period.

It is fortunate that fresh water has its maximum density at about 4°C, since this governs the overturning process and circulation pattern during the cooling period in late fall and early winter. As a result, this warmer and heavier water will reside near the bottom of the water body. Because of this density stratification, conductive heat transfer will dominate the process which is far less effective than the convective process. In introducing air bubbles at the bottom of the water body, extensive water mixing is produced, and the bubbles carry upward a certain amount of warmer water to the surface, to counterbalance the heat loss to the atmosphere.

Many studies have been reported using fluid jets to enhance heat and mass-transfer rates [4–8]. Most of these studies were with single and multiple air jets emerging from slots, holes and nozzles parallel to or impinging normally to the heat-transfer surface. The results are usually expressed in terms of a Nusselt number as functions of a nozzle to plate distance, and Reynolds number based on primarily the slot, hole or nozzle diameter. Sitharamayya and Raju [9] reported the only experimental measurements of heat-transfer characteristics between a submerged water jet and a normal plate. The average heat-transfer coefficient was found to be independent of nozzle to plate distance for $L/d_n < 7$ (d_n is the nozzle diameter).

Little work has been reported regarding the hydrodynamics of the bubble-induced water jet. Based on laboratory experiments using a water tank 2·438 m square and 1·829 m deep, and some elementary analytical considerations, Baines and Hamilton [10] reported that the water flow characteristics of the bubble-driven jet pattern consists of a vertical jet rising from the air source and a thin, horizontal, radially-spreading jet along the surface. The momentum of the vertical jet increases with height from the source. They also reported that the flow pattern is independent of the size of nozzle openings in the range of 0·508 mm or larger, but is a function of the air discharge rate. The ratio of water entrainment to air discharge rate was found to increase with depth and decrease with increasing air discharge. In a recent study, using columns 0·914 m in height and 50·04 mm, 76·2 mm and 0·145 m in diameter, Crabtree and Bridgwater [11] examined analytically and experimentally the liquid motion induced by a chain of rising bubbles through a viscous liquid. The velocity profile and extra pressure drop induced in the liquid by gas bubbling from an opening at the center of the column base were found to be in excellent agreement with a model of the flow which supposes the gas to be equivalent to an upward vertical line of forces along the axis of the cylinder. The most comprehensive work on the analysis of the flow induced by air-bubble systems was reported by Kobus [12]. The analytical treatment considering the momentum-flux increase, due to the buoyancy of the air together with experimental information about the spread of the velocity profiles and the mean rising speed of the air bubble stream, leads to a complete description of the flow field.

To the best of the author's knowledge, no prior

laboratory work has been done regarding the heat-transfer characteristics of a bubble-driven jet impinging on an ice surface. This work is also considered to be useful in destratification of lakes and artificial water reservoirs in control and upgrading of our water resources. The present study investigated the problem experimentally. The effect of column height, diameter, and air bubbling rate on the rate of heat transfer were determined.

Step-like notches 6·35 mm deep were cut into the top of the column to support the ice and maintain it at a proper immersion level during the experiment. Two drain holes 12·7 mm in diameter were located at the desired water level to provide for overflow resulting from the melting. The water circulation in the column purely resulted from bubble motion. The whole column was insulated to minimize the effect of room temperature variation.

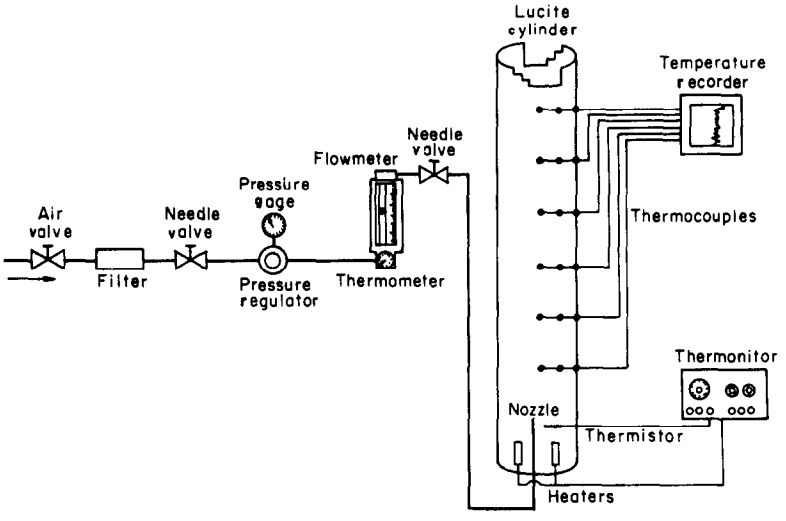

FIG. 1. Schematic of the experimental set-up.

EXPERIMENTAL APPARATUS AND PROCEDURE

Figure 1 shows the schematic diagram of the experimental set-up consisting essentially of a flowmeter, a heating device and a water column. Building air was first filtered through a Lucite cylinder filled with glass-wool, and then passed through a pressure regulator set at $3{\cdot}44 \times 10^4 N/m^2$. A dial thermometer is also attached at the entrance of the flowmeter. From the flowmeter, the air is directed through a copper tube to a check valve rated at $1{\cdot}375 \times 10^4 N/m^2$ before being expelled at the nozzle. The nozzle is a Luer-lok hypodermic needle attached to a connector which is welded onto the end of a copper tube. The nozzle is inserted through the center of the bottom Lucite plate with the tip of the needle about 0·152 m above the plate. Two Lucite columns were used, one 1·829 m high and 0·286 m in diameter and the other 1·219 m high and 0·140 m in diameter. A Cole–Parmer thermistor temperature controller was used to maintain the water temperature at 4°C in the area where the bubbles formed. For the small column a 310 W Hotwatt cartridge heating unit and a thermistor probe were immersed horizontally in the water column just below the nozzle tip. For the large column, three 450 W heating units and a thermistor were positioned vertically through the bottom plate projecting into the column. Eighteen thermocouples were installed at various heights, extending various distances inward from the column wall to measure the water temperature distribution within the column.

Test specimens

The test specimens were cylindrical ice blocks ranging from 0·102 to 0·165 m high and 0·254 to 0·267 m in diameter for the large column; and 0·130 m high and 0·114 m in diameter for the small column. These samples were made from distilled water which had been frozen in an open Lucite cylinder with a copper bottom. Tee-type Lucite supporting devices were partially immersed in the center of the containers during the freezing period and were used in transporting the ice blocks and supporting them at the top of the column during the experiments. The ice was frozen from base upwards by using cold plates with glycol at $-51°C$ as the circulating medium. Ice was formed in this manner to reduce the amount of air bubble entrainment in the ice specimens. When completely frozen, the sample making device was placed in a warm room in an inverted position until the sample slid out from the container. The ice sample was then placed in a cold-room maintained at $-10°C$ to condition it to the same initial temperature before the initiation of an experiment. Copper–constantan thermocouples were used to measure the temperature of the ice sample during each experiment. They were imbedded into holes drilled in the samples and frozen into place, one on top and the others along the sides. The first was located at 38·1 mm from the melting surface (bottom). The second and third were at 63·5 and 88·9 mm high initially.

Prior to any experiment, the column water level was

restored by pouring an appropriate amount of ice cubes in the column. At the same time, the air flow rate was fixed to a specific Rotameter setting. The experimental preparation was carried out until all the ice cubes melted. Then the ice sample, with its dimensions and weight recorded, was lowered into the column and adjusted to about 6·35 mm immersion of the sample bottom below the water level. The time of the initiation of the experiment was recorded.

Bubble frequency and velocity

Bubble frequency and velocity were determined by filming the rising bubbles at various flow rates. A 10·0 × 10·0 mm grid was placed at the rear of the column. A tensor lamp was projected on the grid and a flood lamp was placed at the top of the column to provide adequate lighting. A Kodak-Cine-1600 camera placed on a tripod was used to film the bubbles. The shutter was set at 1/2 open, the lens opening was set at f/2·8, and the film speed was at 64 frames/s. The film used was Eastman Plus-X Negative.

ANALYSIS OF EXPERIMENTAL RESULTS

Three nozzle sizes, i.e. 0·152, 0·406 and 0·838 mm in diameter (d_n) were used in this study. The air flow rates covered the range from $7{\cdot}39 \times 10^{-8}$ to $9{\cdot}91 \times 10^{-7}$ m^3/s. During the experiments, the water temperature throughout the column was found to be almost uniform at 4°C with a decrease of a fraction of a degree from the center toward the wall. The coldroom was maintained at 0+0·2°C. It was frequently observed that the rising air bubbles struck the ice surface at the central portion of the ice cylindrical block and moved radially toward the periphery. It is also important to note that frequently a large bubble formed and covered a great portion of the melting surface, thus retarding the heat transfer. This was because the bottom ice surface became slightly concave due to faster melting in the center impinging region. The remedy was to tip the ice sample a little at regular intervals to facilitate the removal of these large bubbles.

Table 1 summarizes the least square analysis on bubble frequency and velocity. There were slight variations in bubble velocity (v_b); in general v_b increases with the decrease of d_n. For the same large column, v_b shows slight increase with the decrease of the height of the water column (L). The bubble frequency (f_b) was found to increase with the decrease of d_n, and can be satisfactorily related to the Rotameter setting R by an exponential function. For the same value of d_n, in general, the values of f_b are higher in the large column than in the small column. The bubble size is more or less uniform for a given d_n and a given volumetric air flow rate (V_a). However, the bubbles are not spherical in shape. The equivalent bubble diameter (d_b) can be computed from $d_b = (6V_a/f_b\pi)^{1/3}$.

The small column experiments were conducted for a duration of one hour to eliminate or reduce the extent of an uneven melting surface due to excessive melting in the jet impinging region. For the large column, a period of 1½ h or longer was usually used. To insure that the experimental data were representative of steady state conditions, a series of experiments were conducted for a specific air flow rate under various durations. The weight loss of the ice sample (or the extent of melting) was found to vary linearly with the experimental duration.

The heat-transfer coefficient between the melting ice and the bubbling water was evaluated in the following manner: The ice sample was weighed before and after the completion of the experiment, and the weight loss was used to determine the total heat used to melt the ice. The temperature change of the remaining ice sample was also recorded at various distances from the melting surface during the experiment.

The temperature change was a result of the combined effects of heat conducted through the melting surface, and radiation exchange and natural convection between the ice sample and the surroundings. The later effects were determined by suspending the ice sample in the column but not in contact with the water, and recording the temperature rise of the ice for a given experimental duration.

To compute the total upward heat transfer, the enthalpy change of the remaining ice sample and the amount of heat associated with phase changes were evaluated. The net enthalpy change can be approximated by

$$Q_s = M_s c_i (\Delta T_m - \Delta T_{cr}) \tag{4}$$

Table 1. Variation of bubble frequency, velocity as a function of column height, diameter, and nozzle opening

Column height L (m)	Column diameter D (m)	Nozzle opening d_n (mm)	Bubble frequency f_b (bubbles/s)	Bubble velocity v_b (m/s)
0·840	0·140	0·838	2·9604 exp (0·0136R)	0·3157 + 0·00027R
		0·406	11·1455 exp (0·0136R)	0·3520 + 0·00012R
		0·152	25·942 exp (0·0101R)	0·4121 − 0·00034R
1·524	0·286	0·838	3·6946 exp (0·0144R)	0·3573 + 0·00043R
		0·406	7·6411 exp (0·0138R)	0·3570 + 0·00003R
		0·152	33·2515 exp (0·0037R)	0·4066 − 0·00030R
0·762	0·286	0·838	3·5825 exp (0·0150R)	0·3652 + 0·00046R
		0·406	8·4201 exp (0·0123R)	0·4018 − 0·00009R
		0·152	36·4391 exp (0·0024R)	0·4281 − 0·00034R

where M_s is the weight of the ice sample at the completion of the experiment, c_i is the heat capacity of ice, ΔT_m is defined as $(\Delta T_b+\Delta T_t)/2$ where ΔT_b and ΔT_t are the differences between the initial and final ice temperatures near the bottom melting and top ice surface, respectively. ΔT_{cr} is the temperature rise of the ice sample resulting from the combined effects of natural convection and thermal radiation. The heat exchange associated with the melted ice is

$$Q_m = W_i[L_i+(T_f-T_i)c_i] \quad (5)$$

where W_i is the weight of ice melted, L_i is the latent heat of fusion, and T_i is the initial ice temperature. With Q_s and Q_m determined, an average heat-transfer coefficient based on the sample cross-sectional area can be computed:

$$h_s = \frac{Q_s+Q_m}{A\Delta T\theta} \quad (6)$$

where A is the cross sectional area of the ice sample. ΔT is the difference between the bulk water temperature and the melting point of ice and θ is the duration of the experiment.

Due to the lack of information on flow characteristics of the bubble-driven water jet, d_n and the air velocity v_a at the nozzle exit was used to define a Rayleigh number $Re_n(=d_n v_a/\nu_a)$, where ν_a is the kinematic velocity of air evaluated at 4°C. Similarly, a Nusselt number also based on d_n was defined, i.e. $Nu_n = hd_n/k_w$, where k_w is the thermal conductivity of water at 4°C. Table 2 summarizes the experimental parameters covered in this study. The results from the small column with ice

Table 2. Variation of experimental parameters

Column height L (m)	Sample diameter D_s (m)	Nozzle opening d_n (mm)	Ratio of L/d_n	Ratio of D_s/d_n
0·840	0·110	0·838	1000	133
		0·406	2063	273
		0·152	5500	729
1·524	0·280	0·838	1818	310
		0·406	3750	641
		0·152	10 000	1708
0·762	0·260	0·838	909	310
		0·406	1875	641
		0·152	5000	1708

sample diameter $D_s = 0{\cdot}110$ m, and nozzle to ice surface distance $L = 0{\cdot}840$ m are shown in Fig. 2. The experimental value lies fairly well along a straight line on a log–log plot for each d_n. A cross plot of the results shows that for a given Re_n, the Nu_n variation with d_n is as a power function $Nu_n \alpha (d_n)^{1{\cdot}4}$. The results for a large column with $D_s = 0{\cdot}260$ m, and $L = 1{\cdot}524$ are shown in Fig. 3. As demonstrated in Fig. 2, the data also can be fairly represented by straight lines on a log–log plot. Quite a few experiments were also carried out for $L = 0{\cdot}762$ m for $d_n = 0{\cdot}152$ and 0·406 m. There seems to be a trend showing a higher Nu_n value for a given Re_n, but it is felt that there is no sufficient data to warrant a

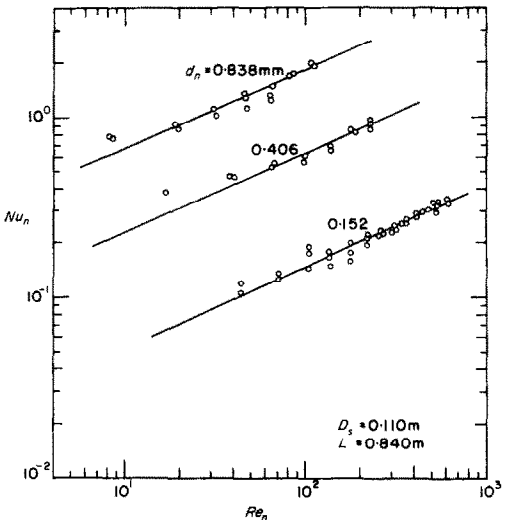

FIG. 2. Relationship between Nu_n and Re_n for $d_n = 0{\cdot}152$, 0·406 and 0·838 mm ($D_s = 0{\cdot}110$ m, $L = 0{\cdot}840$ m).

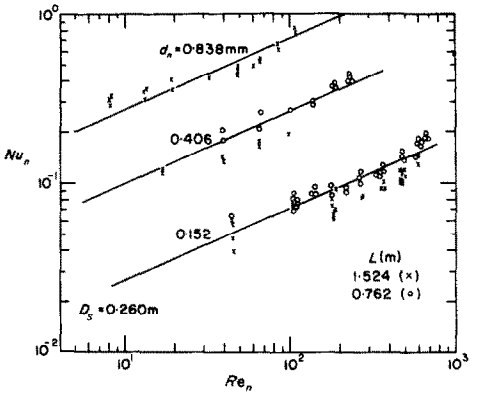

FIG. 3. Relationship between Nu_n and Re_n for $d_n = 0{\cdot}152$, 0·406 and 0·838 mm ($D_s = 0{\cdot}260$ m, $L = 0{\cdot}762$ and 1·524 m).

conclusion. A cross plot of this result also gives a Nu dependence on d_n by the relation $Nu_n \alpha (d_n)^{1{\cdot}4}$. Subsequently, using $Nu_n/(d_n)^{1{\cdot}4}$ as ordinate, all the data (64 for $D_s = 0{\cdot}110$ m, and 107 for $D_s = 0{\cdot}260$ m) were plotted in Fig. 4. The least square analysis gave correlation

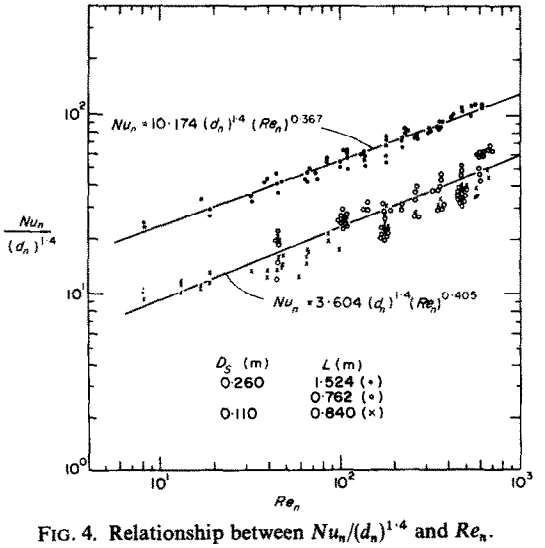

FIG. 4. Relationship between $Nu_n/(d_n)^{1{\cdot}4}$ and Re_n.

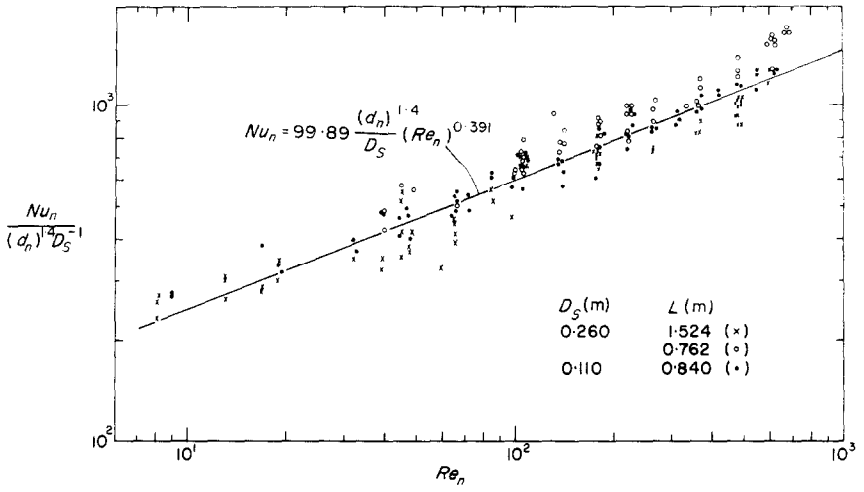

FIG. 5. Relationship between $Nu_n/(d_n)^{1\cdot4}(D_s)^{-1}$ and Re_n.

coefficients 0·976 for $D_s = 0{\cdot}110$ m and 0·936 for $D_s = 0{\cdot}260$ m, with corresponding slopes of 0·367 and 0·354 respectively. Since the effect of L is not significantly demonstrated in our limited data, the effect of D_s was subsequently evaluated by a cross plot of Fig. 4. The dependence of $Nu_n/(d_n)^{1\cdot4}$ on D_s was found to be $Nu_n/(d_n)^{1\cdot4} \alpha D_s^{-1}$. All the results as shown in Fig. 5 can be well represented by

$$Nu_n = 99{\cdot}89(d_n)^{1\cdot4}(D_s)^{-1}(Re_n)^{0\cdot391} \quad (7)$$

with a correlation coefficient of 0·947, in which d_n and D_s are in centimeters. In terms of D_s and expressing D_s and d_n in meters, equation (7) can be transformed to

$$Nu = 630(d_n)^{0\cdot4}(Re_n)^{0\cdot391} \quad (8)$$

in which $Nu = hD_s/k_w$.

DISCUSSION

To the best of the author's knowledge, no work of a similar nature involving the hydrodynamics and the heat-transfer characteristics between an air-bubble driven jet and a surface held at normal has been reported. In fact, very little study has been done on the flow characteristics on the water jet induced by the rising bubble stream. In Crabtree and Bridgwater's study using glycerol as the fluid and at a much slower bubble rise velocity in the order of 40–55 mm/s, they developed the following velocity function

$$v = \frac{G}{2\pi\mu}\left[\left(\frac{r^2}{R^2}\right) + \ln\left(\frac{R}{r}\right) - 1\right]. \quad (9)$$

In which G is the force per unit height imposed on the liquid, r is the radial distance from column axis, μ is the liquid viscosity, and R is the column radius. This experiment was compared with their experimental data and was found to be in excellent agreement. From equation (9), it can be calculated that at $r = 0{\cdot}45R$, $v = 0$. Therefore there are two flow regions, an upward flow when $r \leqslant 0{\cdot}45R$, and downward flow region when $r > 0{\cdot}45R$. However, it is doubtful that this finding can be used to describe the flow characteristics of the bubble-driven jet. The work of Sitharamayya and Raju [9] on heat transfer between a submerged jet of water and a flat surface held normal to the flow was much closer to the conditions of the present study. They present their final correlation as

$$(Nu_n Pr^{-0\cdot33})\left(\frac{D_s}{d_n}\right)^2 = 32{\cdot}49(Re_n)^{0\cdot523} + 0{\cdot}266[(D_s/d_n) - 8](Re_n)^{0\cdot828} \quad (10)$$

for Re_n ranging from 2000 to 40 000 and for $L/d_n < 7$, and $8 \leqslant (D_s/d_n) \leqslant 58$ with both Nu_n and Re_n defined based on d_n as in the present analysis in which D_s is the diameter of the heat-transfer surface. Because the parameter L/d_n used is much smaller than the present case, this work can not be used for comparison (see Table 2).

The work of Kobus [12] was conducted in an $8 \times 280 \times 4{\cdot}70$ m basin and is again only interested in the hydrodynamic aspect of the problem. He found the pattern of vertical velocity induced by an orifice discharging air into water can be presented by Gaussian distribution curves with a linear spread in the vertical except for the regions near the orifice and close to the free surface. The velocity distribution was expressed as

$$\frac{v_w}{v_c} = \exp\left(\frac{-r^2}{2C^2(L+y_0)^2}\right) \quad (11)$$

in which v_w and v_c are vertical and arrival or axial velocity, C is the rate of spread of velocity profiles. The expression for v_c was derived as

$$v_c = \frac{1}{C(L+y_0)}\left[\frac{-p_{atm}}{\pi\rho_w v_b}\ln\left(1 - \frac{L}{L^*}\right)\right]^{1/2} \quad (12)$$

where v_b is mean rising speed of air bubble stream, L^* is the sum of L and p_{atm}/γ (γ is the specific weight of water), L is the vertical distance above air source, and y_0 is the analytical origin resulting from an analytical extension of the established flow pattern into and beyond the limits of the initial region. This origin does not coincide with the location of the air source because of the markedly different conditions in the initial region.

From his experimental study, he reported that both spread coefficient C and v_b can be represented by

$$C = C_c(V_a)^{0.15} \tag{13}$$

and

$$v_b = C_b(V_a)^{0.15}. \tag{14}$$

From his experimental results the values of C_c and C_b are found to be $C_c = 0.133(m^{-0.3}s^{0.15})$ and $C_b = 1.84(m^{0.55}s^{-0.85})$.

In the work reported by Gardon and Akfirat [5], the following correlation was given for single round air jets impinging centrally on circular targets of diameter D_s.

$$Nu = 0.78(Re_a)^{0.55}. \tag{15}$$

Provided $Re_a > 4000$, $L/d_n > 12$, and $1 < D_s/d_n < 24$ in which Nu is defined as hD_s/k_w and Re_a as $D_s v_c/\nu_w$. By analogy with other turbulent heat transfer, it is expected that $Nu \propto Pr^{1/3}$. Assuming $Pr = 0.7$ for air and $Pr = 11.7$ for water at 4°C, equation (15) can be transformed to apply to water flow in the form

$$Nu = 1.94(Re_a)^{0.55}. \tag{16}$$

Extending Kobus's results to a confined cylindrical column, the diameter at impingement is

$$D_i = 2C(L + y_0) \tag{17}$$

or

$$D_i = 2C_c(L + y_0)(V_a)^{0.15} \tag{18}$$

where the value of y_0 as reported by Kobus is taken as 0.8 m, V_a is the volumetric air flow rate at nozzle exit at atmospheric conditions. With v_b evaluated from equation (14), the value of v_c can be computed from equation (12).

With the value of v_c and D_i thus determined and the given value of ν_w, the Reynolds number describing the flow characteristics of the bubble-induced water jet can be evaluated. Corresponding Nusselt numbers based on D_i were also computed. The log–log plot of Nu_i vs Re_i is shown in Fig. 6 along with equation (16).

It is clear that the experimental results are higher than those predicted from equation (16). It also shows clearly that the shorter the column height, the higher the values of Nu_i for the same D_s. This is from the fact that for the same air flow rate, the value of D_i is lower for the lower water level (see equation (18)), and the value of Nu_i is inversely proportional to the first power of D_i. In all cases, the calculated values of D_i are much smaller than D_s. The ratio of D_i/D_s was found to vary from 0.135 to 0.201 at $L = 0.762$ m and from 0.200 to 0.300 at $L = 1.524$ m for the large column, and from 0.335 to 0.492 at $L = 0.840$ m for the small column for volumetric discharge rate ranging from 7.39×10^{-8} to 9.91×10^{-7} m^3/s. In computing the value of heat-transfer coefficient in Nu_i shown in Fig. 6, the area corresponding to D_i and the total amount of heat exchange ($Q_s + Q_m$) were used. Since the ratio of D_i/D_s varies with both V_a and D_s, and represents only about 4, and 9 per cent of the sample surface area A for the large column, and 25 per cent of the small column, it is reasonable to expect the results from the small column were closer to those predicted from equation (16). However, from observations at the completion of an experiment, the melting ice surface is more or less even, indicating uniform melting across the sample surface for low to medium V_a. For higher V_a, the resultant melting surface does show a slight concave upward, exhibiting a faster melting rate near the jet impingement region. To have a better comparison with equation (16), one would have to evaluate the effective heat-transfer area more accurately, and this can only be done by measuring the flow field near the melting surface.

Also the conditions given in equation (16) are not exactly met. In our case, the Reynolds numbers are ranging from 1.4 to 5.5×10^3 with a majority of Re_i less than 4.0×10^3. In regard to the condition $1 < D_s/d_n < 24$, we have the range $42 < D_i/d_n < 510$. However, as it can be noted in Fig. 6, the value of Nu_i has a dependence of Re_i with an exponent close to 0.55 as in equation (16). Furthermore, using v_c to define the Reynolds number, the effect of d_n disappeared.

Since the topography of the melting surface was quite smooth and even at the completion of the experiment (especially for low V_a values), the heat-transfer coefficient based on the sample area was used in defining Nu, and D_s instead of D_i used in defining Re_a. The results are shown in Fig. 7 along with equation (16). As shown

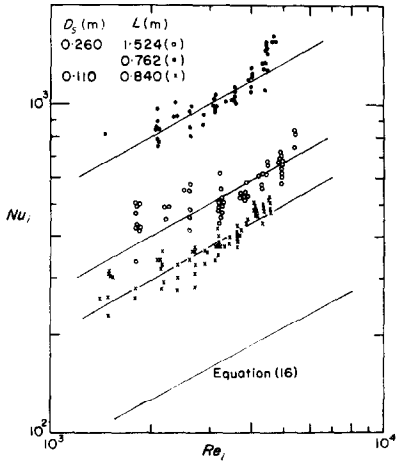

FIG. 6. Relationship between Nu_i and Re_i.

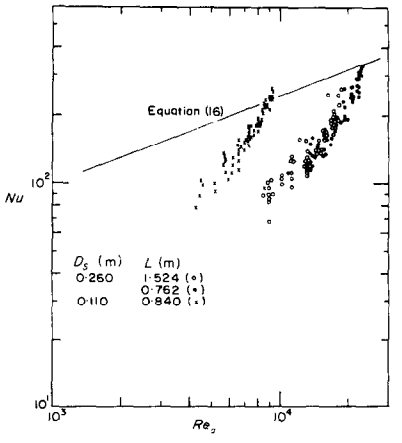

FIG. 7. Relationship between Nu and Re_a.

in Fig. 6, there is no effect of d_n in such a correlation. Furthermore the effect of L for the same column diameter, D is insignificant. However, the effect of D_s is clearly demonstrated. The results indicate that generally the experimental values are lower than those predicted from equation (16), but with a much stronger dependence of Nu on Re_a, therefore at higher Re_a the experimental values are higher than those from equation (16).

In light of the restriction imposed in equation (16), the agreement was found to be good. Since the log–log plot of the data for the two D_s are indeed linear and parallel, a cross-plot showing Nu vs Re_a resulting in a dependency of $Nu \propto (D_s)^{-1\cdot2}$. Thus all the data can be correlated as

$$Nu = 0{\cdot}00010(D_s)^{-1\cdot2}(Re_a)^{1\cdot311} \qquad (19)$$

in which D_s is expressed in meters.

CONCLUSIONS

In all, 171 experiments were conducted using three nozzle sizes, i.e. 0·132, 0·406 and 0·838 mm dia. Two Lucite columns, 0·140 and 0·286 m in diameter, were used. In the large column, two sets of data were taken for water column height at 0·762 and 1·524 m. On the other hand, only one height, 0·840 m, was used in the small column. All the data as shown in Fig. 5 can be rewritten as

$$Nu = 630(d_n)^{0\cdot4}(Re_n)^{0\cdot391}$$

with d_n expressed in meters and a correlation coefficient of 0·947. It was found that for the air flow range covered in this study, the effect of L on heat transfer was found to be insignificant.

To compare with data given for round air jets impinging on a plane surface held normal to the jet, a correlation like

$$Nu = 0{\cdot}00010(D_s)^{-1\cdot2}(Re_a)^{1\cdot311}$$

can be presented with a correlation coefficient of 0·983. In Re_a, the centerline axial water velocity was used. In arriving at this correlation (as shown in Fig. 7), the effect of d_n and L were not present. However the effect of D_s was clearly demonstrated in Fig. 7. Due to lack of research in regard to the hydrodynamics and heat-transfer characteristics of a bubble-driven jet, no analytical expression can be served as a basis for comparison with the present experimental results.

Acknowledgement—Sponsorship of this work by the In-House Laboratory Independent Research Program at the U.S. Army Cold Regions Research and Engineering Laboratory is greatly appreciated. The author wishes to thank Messrs. Anthony Zehnder and Roy Yoshimoto for conducting some of the experiments.

REFERENCES

1. A. Davis, Protection of Keokuk Dam gates from ice pressure by the use of air, *Stone and Webster J.* **22**, 199–206 (1918).
2. G. P. Williams, A study of winter temperatures and ice prevention by air bubbling, *Engng J.* **44**, 79–84 (1961).
3. B. Michel, Winter regime of rivers and lakes, Cold Regions Sciences and Engineering monograph II-Bla, U.S. Army Cold Regions Research and Engineering Laboratory, Hanover, NH (1971).
4. M. J. Symons, Water quality behaviors, Public Health Service Publication No. 1930, U.S. Dept. of H.E.W. Bureau of Water Hygiene, Cincinnati, Ohio (1969).
5. R. Gardon and J. C. Akfirat, Heat transfer characteristics of impinging two-dimensional air jets, *J. Heat Transfer* **88C**, 101–108 (1966).
6. S. J. Friedman and A. C. Muller, Heat transfer to flat surfaces, Proc. general discussion on heat transfer, *Proc. Instn Mech. Engrs* 138–142 (1951).
7. J. M. F. Vickers, Heat transfer coefficients between fluid jets and normal surface, *Ind. Engng Chem.* **51**, 967–972 (1959).
8. R. Gardon and T. Cobonpue, Heat transfer between a flat plate and jets of air impinging on it, *Int. Dev. Heat Transfer*, pp. 454–460. A.S.M.E., New York (1963).
9. S. Sitharamayya and K. S. Raju, Heat transfer between an axisymmetric jet and a plate held normal to the flow, *Can. J. Chem. Engng* **47**, 365–368 (1969).
10. W. D. Baines and G. F. Hamilton, On the flow of water induced by a rising column of air bubbles, *Proc. 8th Cong. of the Inst. Assoc. of Hydr. Res.* Vol. 2, paper 7-D (1959).
11. J. R. Crabtree and J. Bridgwater, Chain bubbling in viscous liquids, *Chem. Engng Sci.* **24**, 1755–1768 (1969).
12. Helmut E. Kobus, Analysis of the flow induced by air-bubble system, *Coast Eng. Conf.* Vol. II, London, Chapter 65, pp. 1016–1031 (1968).

CARACTERISTIQUES DU TRANSFERT THERMIQUE D'UN JET D'EAU INDUIT PAR DES BULLES D'AIR ET FRAPPANT UNE SURFACE DE GLACE

Résumé—Une étude expérimentale a été effectuée sur les caractéristiques du transfert de chaleur d'un jet d'eau induit par des bulles d'air et frappant une surface de glace. Deux colonnes Lucite, l'une de 1,829 m de haut sur 0,286 m de diamètre et l'autre de 1,219 m de haut sur 0,140 m de diamètre ont été utilisées. Les niveaux d'eau ont été maintenus à 0,762 et 1,524 m dans la grande colonne et 0,840 m dans la petite colonne. Des aiguilles hypodermiques d'ouverture 0,152; 0,406 et 0,838 mm ont été utilisées pour la formation des bulles permettant d'obtenir des débits volumiques d'air allant de $7{,}39 \cdot 10^{-8}$ à $9{,}91 \cdot 10^{-7}$ m^3/s. Afin de simuler les conditions de l'environnement hivernal en Amérique du Nord, la température de l'eau au fond de la colonne a été maintenue par un dispositif thermostatique à sa valeur correspondant à la densité maximale c'est à dire environ 4°C. Des blocs de glace cylindriques de diamètre légèrement inférieur à celui des colonnes, étaient placés au sommet de la colonne en maintenant une immersion convenable de la surface en fusion par rapport au niveau de l'eau. Les résultats expérimentaux peuvent bien être représentés par

$$Nu = 630(d_n)^{0,4}(Re_n)^{0,391}$$

pour $8 < Re_n < 10^3$. Le nombre de Nusselt Nu est défini en fonction du coefficient de transfert de chaleur sur une section droite type, le diamètre et la conductivité thermique de l'eau, et le nombre de Reynolds Re_n est défini en fonction des caractéristiques de l'écoulement d'air à l'embouchure. Les effets de la hauteur des niveaux d'eau et du diamètre de la colonne ont été trouvés absents dans la corrélation.

Utilisant un nombre de Reynolds basé sur les caractéristiques de l'écoulement du jet d'eau induit par les bulles d'air, les résultats expérimentaux ont été comparés aux resultats limites données sur le transfert de chaleur entre un jet d'air circulaire et une surface plane maintenue normalement à l'écoulement (modifiés afin de s'appliquer à un écoulement d'eau). L'expression obtenue par optimisation au sens des moindres carrées,

$$Nu = 0{,}00010(D_s)^{-1{,}2}(Re_a)^{1{,}311}$$

qui indique l'absence du diamètre de l'embouchure et la hauteur du niveau d'eau, s'est avérée représenter extrêmement bien les données. L'expression ci-dessus sous-estime et sur-estime le nombre de Nusselt Nu pour des valeurs de Re_a inférieures et supérieures à celles prévues par la relation pour un jet d'eau pure $Nu = 1{,}94(Re_a)^{0{,}55}$. Cependant considérant les nombreuses hypothèses et les grandes variations dans les paramètres expérimentaux, l'accord est encore considéré comme remarquablement bon.

WÄRMEÜBERGANG EINES DURCH BLASEN INDUZIERTEN WASSERSTRAHLS BEIM AUFTREFFEN AUF EINE EISOBERFLÄCHE

Zusammenfassung—Es wurde experimentell der Wärmeübergang eines durch Blasen erzeugten Wasserstrahls beim Auftreffen auf eine Eisfläche untersucht. Zwei senkrecht aufgestellte Plexiglasrohre, das eine mit 1,829 m Höhe und 0,286 m lichtem Durchmesser, das andere mit 1,219 m Höhe und 0,140 m lichtem Durchmesser, wurden untersucht. Der Wasserspiegel wurde auf knostanter Höhe bei 0,762 m im großen Rohr und bei 0,840 m im kleinen Rohr gehalten. Zur Erzeugung der Blasen wurden Injektionskanülen mit Öffnungen von 0,152, 0,406 und 0,838 mm benutzt; damit erhält man einen Volumenstrom der Luft zwischen $7{,}39 \times 10^{-8}$ und $9{,}91 \times 10^{-7}$ m³/s. Um nordamerikanische Winter-Umgebungsbedingungen zu simulieren, wurde die Wassertemperatur am Rohrboden mit einem Thermostaten auf der Temperatur maximaler Dichte, in diesem Fall etwa 4°C gehalten. Zylindrische Eisblöcke, deren Durchmesser etwas kleiner als die der Rohre waren, wurden oben in das Rohr gegeben, wobei eine geeignete Eintauchtiefe der zerschmelzenden Oberfläche im Wasserbeibehalten wurde. Die experimentellen Ergebnisse können gut wiedergegeben werden mit

$$Nu = 630(d_n)^{0{,}4}.(Re_n)^{0{,}391}$$

wobei $8 < Re_n < 10^3$ ist. Die Nusselt–Zahl ist definiert mit dem Wärmeübergangskoeffizienten über die Querschnittsfläche der Probe, mit dem Probendurchmesser und der Wärmeleitfähigkeit des Wassers. Die Re–Zahl ist definiert mit den Daten des Luftstroms am Düsenaustritt. Ein Einfluß der Höhe des Wasserspiegels und des Rohrdurchmessers konnte nicht festgestellt werden. Es wurde eine Re–Zahl mit der Charakteristik des durch Blasen induzierten Wasserstrahls definiert und die experimentellen Ergebnisse verglichen mit den im begrenzten Umfang zur Verfügung stehenden Ergebnissen des Wärmeübergangs zwischen einem runden Luftstrahl und einer ebenen Oberfläche, die senkrecht zu diesem Strahl gehalten wird (in modifizierter Form auf einen Wasserstrahl anzuwenden). Der Ausdruck mit dem kleinsten Fehlerquadrat

$$Nu = 0{,}00010(D_3)^{-1{,}2}(Re_a)^{1{,}311}$$

in den der Düsendurchmesser und die Höhe des Wasserspiegels nicht eingehen, ergab eine sehr gute Übereinstimmung mit den gemessenen Daten. Mit dieser Beziehung bestimmt man zu kleine und zu große Werte der Nu–Zahl für niedrige und höhere Re–Zahlen gegenüber denen, die man mit der Beziehung $Nu = 1{,}94.(Re_a)^{0{,}55}$ für einen reinen Wasserstrahl berechnet. In Anbetracht der zahlreichen Vernachlässigungen und der starken Unterschiede der experimentellen Parameter ist die Übereinstimmung noch als bemerkenswert gut zu bezeichnen.

ХАРАКТЕРИСТИКИ ТЕПЛОПЕРЕНОСА ИНДУЦИРОВАННОГО ПУЗЫРЬКАМИ ОТ СТРУИ ВОДЫ, ПАДАЮЩЕЙ НА ПОВЕРХНОСТЬ ЛЬДА

Аннотация — Проводилось экспериментальное исследование характеристик теплообмена, индуцированного пузырьками от струи воды, падающей на поверхность льда. Использовались колонны типа Люсит, одна высотой 1,829 м и диаметром 0,286 м, а другая высотой 1,219 м и диаметром 0,140 м. Вода поддерживалась на уровне 0,762 и 1,524 м в большой колонне и 0,840 м в меньшей. Для образования пузырьков пара использовались инъекционные иглы с отверстиями 0,152, 0,406 и 0,838 мм при объемном расходе воздуха от $7{,}39 \times 10^{-8}$ до $9{,}91 \times 10^{-7}$ м³/сек. В целях иммитирования зимних условий окружающей среды в Северной Америке, температура воды на дне колонны термостатически поддерживалась при температуре максимальной плотности, т. е. около 4°C. Цилиндрические блоки льда с диаметром несколько меньшим, чем диаметр колонны, загружались сверху колонны, тем самым поддерживая соответствующее погружение тающей поверхности в воду. Экспериментальные результаты могут быть хорошо представлены

$$Nu = 630(d_n)^{0{,}4}(Re_n)^{0{,}391}$$

для $8 < Re_n < 10^3$. Число Нуссельта определялось через коэффициент теплопереноса на площади поперечного сечения образца; диаметр образца и теплопроводность воды и Re_n определялись через характеристики потока воздуха на входе в сопло. При обобщении данных найдено, что отсутствует влияние как уровней воды, так и диаметра. С помощью числа Рейнольдса для

гидродинамических характеристик индуцированной пузырьками струи воды проводилось сравнение экспериментальных результатов с ограниченными данными по теплообмену между круглой струей воздуха и плоской поверхностью, перпендикулярной к потоку струи (модифицированные для потока воды).

Выражение, полученное методом наименьших квадратов

$$Nu = 0{,}00010(D_s)^{-1{,}2}(Re_a)^{1{,}311}$$

при отсутствии влияния как диаметра сопла, так и высоты уровня воды, показывает исключительно хорошее согласование данных. Вышеуказанное выражение дает завышенные и заниженные значения числа Нуссельта для меньших и больших значений Re_a по сравнению со значениями, полученными из выражения для чистой струи воды $Nu = 1{,}94(Re_a)^{0{,}55}$. Однако, учитывая многочисленные допущения и большие различия в экспериментальных параметрах, согласование данных по-прежнему может считаться исключительно хорошим.